

Above-ground woody carbon sequestration measured from tree rings is coherent with net ecosystem productivity at five eddy-covariance sites

Flurin Babst^{1,2}, Olivier Bouriaud³, Dario Papale⁴, Bert Gielen⁵, Ivan A. Janssens⁵, Eero Nikinmaa⁶, Andreas Ibrom⁷, Jian Wu⁷, Christian Bernhofer⁸, Barbara Köstner⁸, Thomas Grünwald⁸, Günther Seufert⁹, Philippe Ciais¹⁰ and David Frank^{1,11}

¹Swiss Federal Research Institute WSL, Zürcherstrasse 111, 8903 Birmensdorf, Switzerland; ²Laboratory of Tree-Ring Research, University of Arizona, 1215 E Lowell St., Tucson, AZ 85721, USA; ³Forest Research and Management Institute ICAS, Sos. Stefanesti 128, O77190 Voluntari, Romania; ⁴Department for Innovation in Biological, Agro-Food and Forest Systems, University of Tuscia, Via S. Camillo de Lellis, 01100 Viterbo, Italy; ⁵University of Antwerp, Universiteitsplein 1, 2610 Wilrijk, Belgium; ⁶Department of Physics, University of Helsinki, PO Box 9, FIN-00014 Helsinki, Finland; ⁷Department of Chemical and Biochemical Engineering, Technical University of Denmark (DTU), Frederiksborgvej 399, Roskilde, Denmark; ⁸Technical University of Dresden, Piener Strasse 23, 01737 Tharandt, Germany; ⁹EC-JRC, Institute for Environment and Sustainability, Via Fermi 2749, 21027 Ispra, Italy; ¹⁰Laboratoire des Sciences du Climat et de L'Environnement, CEA-CNRS-UVSQ, F-91191, Gif-sur-Yvette, France; ¹¹Oeschger Center for Climate Change, Zähringerstr. 25, 3012 Bern, Switzerland

Summary

Author for correspondence:

Flurin Babst

Tel: +1 520 373 3587

Email: babst@email.arizona.edu

Received: 11 August 2013

Accepted: 3 October 2013

New Phytologist (2013)

doi: 10.1111/nph.12589

Key words: biomass, biometry, carbon allocation, carbon cycle, carbon sink, flux tower, forest productivity, wood density.

- Attempts to combine biometric and eddy-covariance (EC) quantifications of carbon allocation to different storage pools in forests have been inconsistent and variably successful in the past.
- We assessed above-ground biomass changes at five long-term EC forest stations based on tree-ring width and wood density measurements, together with multiple allometric models. Measurements were validated with site-specific biomass estimates and compared with the sum of monthly CO₂ fluxes between 1997 and 2009.
- Biometric measurements and seasonal net ecosystem productivity (NEP) proved largely compatible and suggested that carbon sequestered between January and July is mainly used for volume increase, whereas that taken up between August and September supports a combination of cell wall thickening and storage. The inter-annual variability in above-ground woody carbon uptake was significantly linked with wood production at the sites, ranging between 110 and 370 g C m⁻² yr⁻¹, thereby accounting for 10–25% of gross primary productivity (GPP), 15–32% of terrestrial ecosystem respiration (TER) and 25–80% of NEP.
- The observed seasonal partitioning of carbon used to support different wood formation processes refines our knowledge on the dynamics and magnitude of carbon allocation in forests across the major European climatic zones. It may thus contribute, for example, to improved vegetation model parameterization and provides an enhanced framework to link tree-ring parameters with EC measurements.

Introduction

Forest growth ranks amongst the most important processes that determine the carbon balance of terrestrial ecosystems. The magnitude and dynamics of the forest carbon sink strongly depend on carbon allocation to different storage pools (Litton *et al.*, 2007) and their responses to key determinants, such as climate (Babst *et al.*, 2013), land use change (Kaplan *et al.*, 2012), tree age (Genet *et al.*, 2010), forest disturbances (Kurz *et al.*, 2008; Amiro *et al.*, 2010), management practices (Kowalski *et al.*, 2004; Fahey *et al.*, 2009), nutrient and light competition (Wolf *et al.*, 2011; Sardans & Penuelas, 2013) and intensive seed production

(i.e. masting years in broadleaf species; Mund *et al.*, 2010). These mechanisms form a complex set of drivers for carbon allocation, which is still relatively poorly understood at large scales (Brüggenmann *et al.*, 2011). In particular, the mechanisms linking photosynthesis and carbon storage with above- and below-ground tree growth and ecosystem respiration remain uncertain (Kuptz *et al.*, 2011). In this regard, integrative studies are needed to better constrain the amount of CO₂ captured by different forest carbon pools, and to determine how these pools interact and vary across different spatiotemporal scales.

Since pioneer measurements of turbulent fluxes over tall vegetation, eddy-covariance (EC) has been widely used as a standard

method for the estimation of seasonal fluctuations in carbon exchange between forest ecosystems and the atmosphere (Baldocchi, 2003). In conjunction with forest inventories (Etzold *et al.*, 2011), EC data have greatly improved the understanding of the terrestrial carbon budget and its climate sensitivity at local to global scales (Baldocchi, 2003; Reichstein *et al.*, 2007). Flux towers, however, essentially provide integral measurements above the canopy and leave uncertainties concerning the magnitude and inter-annual variability of carbon allocation within the respective ecosystems. Furthermore, the fraction of CO₂ entering different long-term storage pools is challenging to quantify (Litton *et al.*, 2007; Luyssaert *et al.*, 2007) and may not be constant in time (Campioli *et al.*, 2011) or across ecosystems (Pan *et al.*, 2011). A combination of biometric and EC-based forest productivity assessments could theoretically help to overcome these limitations, but local studies have been variably successful in linking tree growth and carbon stock changes (i.e. allocation of photosynthates to wood production) with flux tower measurements (Barford *et al.*, 2001; Curtis *et al.*, 2002; Gough *et al.*, 2008; Gielen *et al.*, 2013). Conclusions ranged from finding nearly no link to observing high coherence between biometric and EC data. For example, Rocha *et al.* (2006) found no significant relationship between tree-ring width (TRW) chronologies from selected mature black spruce (*Picea mariana*) trees and annual ecosystem carbon gain in central Canada. By contrast, Zweifel *et al.* (2010) reported remarkably close links between stem radius changes and gross primary productivity (GPP) at hourly to inter-annual time-scales in a Swiss subalpine Norway spruce (*Picea abies*) forest, driven by a combination of growth, stem water balance and frost-induced shrinkage. Ohtsuka *et al.* (2009) observed a significant relationship of net ecosystem productivity (NEP) with woody biomass increment, but not with foliage production, at a central Japanese flux site. Results from these and other studies hint at the complexity of the processes and ecosystems under question, especially as wood formation is additionally supported by stored carbohydrate reserves (Richardson *et al.*, 2013). Ilvesniemi *et al.* (2009) found reasonable agreement between tree-ring and EC-based productivity estimates in a Scots pine (*Pinus sylvestris*) forest in southern Finland. Yet, decreasing coherence with increasing distance between sampled trees and the flux tower suggest rather local representation of these data. Granier *et al.* (2008) found high correlations between biometric and EC estimates at weekly to monthly time-scales in a young beech (*Fagus sylvatica*) stand in northern France. The disappearance of these links in the second half of the growing season, and thus at annual time-scales, suggests that the timing of wood formation plays a key role in the quantification of forest carbon assimilation. Given the current state of literature on biometric and EC comparisons, it is premature, if not impossible, to make generalizations with regard to the complementarity and compatibility of these two different ecosystem perspectives. Comparable investigations at multiple flux tower sites across different biomes are needed.

Above-ground woody biomass increment in trees can be calculated as the product of the volume increase and wood density. All existing biometric studies rely on stem diameter changes derived

from tree rings (Rocha *et al.*, 2006), dendrometer data (Zweifel *et al.*, 2010) or repeated inventories of tree girth (Ohtsuka *et al.*, 2007). Some studies (Wirth *et al.*, 2004; Wutzler *et al.*, 2008) additionally consider tree height to avoid a priori and potentially site-specific parametric relationships between diameter and stem volume. Wood density is generally assumed to be constant in biomass assessments, thereby neglecting its inter-annual to centennial variation owing to both climate and tree age (Bouriaud *et al.*, 2004). The extent to which changes in wood density and its between-tree variability induce errors into local (Ilvesniemi *et al.*, 2009) to national (Nepal *et al.*, 2012) forest carbon inventories remains unclear. Investigations of TRW and maximum latewood density have shown that these parameters are most sensitive to environmental conditions during different times of the year (Briffa *et al.*, 2002; Frank & Esper, 2005). We thus hypothesize that different climatic controls apply to radial growth and average ring density (XD), and therefore the variability of both is needed to accurately estimate the annual biomass increment in trees.

Tree-ring analyses permit fully compatible measurements of TRW and XD from the same samples, and are thus a valuable archive of annually resolved variability in stem biomass (Bouriaud *et al.*, 2004) and growth over inter-annual (Babst *et al.*, 2012a) to centennial (Esper *et al.*, 2002) time-scales. Large TRW networks have been compiled to address forest growth variability on continental scales (Gedalof & Berg, 2010; Babst *et al.*, 2013). These datasets, however, are not suitable to infer stand biomass changes. As outlined in Babst *et al.* (2012b), there is little control concerning the number of trees, their dimensions and social status, the research area or even which trees from a stand were sampled. This information is required to transform tree-ring parameters into biomass increments using allometric biomass functions (Zianis *et al.*, 2005; Tabacchi *et al.*, 2011). Furthermore, sample collection is usually oriented towards individual project goals and may influence or even severely bias the quantification of growth variability (Melvin, 2004).

Aiming to reconcile the quantification of carbon cycling from biometric and EC techniques, we measured radial tree growth and wood density at five long-term EC forest sites. The resulting records were used to calculate the annual above-ground woody biomass increment (i.e. stems and branches) and associated carbon uptake. We corrected tree-level biomass increments for inter-annual variations in wood density before upscaling to stand-level carbon uptake in above-ground woody tissues. Inter-annual growth variability was verified with neighboring tree-ring chronologies (Babst *et al.*, 2013) to test the spatial representativeness of individual sites. Subsequent comparisons with the sum of monthly to seasonal CO₂ flux measurements (i.e. NEP) and derivatives thereof (GPP; terrestrial ecosystem respiration, TER) were performed to assess: (1) the seasons in which EC and tree-ring data correspond best in different parts of Europe; and (2) the fraction of eddy fluxes that is associated with changes in above-ground woody carbon stocks. Our efforts contribute to reducing the uncertainties in estimates of the carbon allocation processes in forested ecosystems.

Materials and Methods

Study sites

Trees were sampled from five CO₂ flux monitoring forest sites (Fig. 1) equipped with continuous and long-term measurements of net ecosystem CO₂ exchange. The study sites are all part of the FLUXNET network and include Hyytiälä (FI-Hyy), Sorø (DK-Sor), San Rossore (IT-SRo), Tharandt (DE-Tha) and Braschaat (BE-Bra). FI-Hyy is located in a boreal Scots pine (*Pinus sylvestris* L.) forest in central Finland next to Lake Kuivajärvi, and is characterized by short summers, cold winters and relatively low annual precipitation (Table 1). DK-Sor is situated in a beech (*Fagus sylvatica* L.) stand in central Zealand (Denmark), where the temperature amplitude and precipitation seasonality are relatively low throughout the year. IT-SRo represents a northern Mediterranean climate with hot and dry summers and mild and humid winters. Maritime pine (*Pinus pinaster* Aiton.) is the dominant species at this near-sea site in Tuscany (Italy), which experiences harsh growth conditions from sandy soils and strong winds from the sea (trees are tilted landwards). DE-Tha is located in a mixed forest in eastern Germany, where precipitation amounts are highest during the June–August season and the temperature amplitude throughout the year is rather large. Norway spruce (*Picea abies* Karst.) is the dominant species at this site. BE-Bra lies in Flanders (Belgium) and represents a temperate maritime climate with mild summers and winters, as well as evenly distributed rainfall throughout the year. The forest is composed of

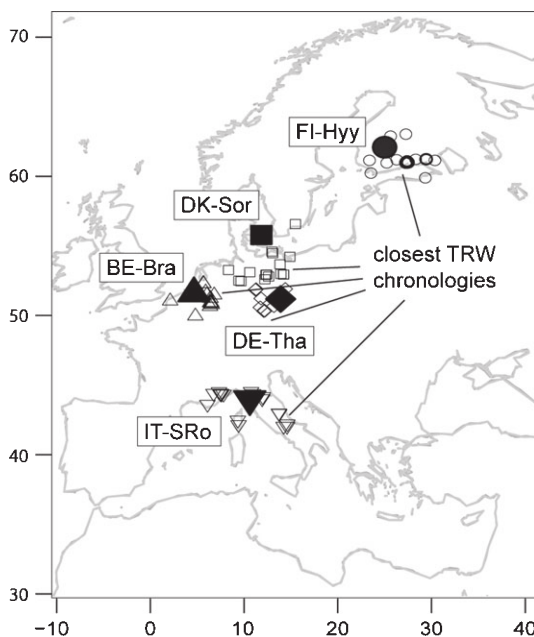


Fig. 1 Location of five flux tower sites in Hyytiälä (FI-Hyy), Sorø (DK-Sor), San Rossore (IT-SRo), Tharandt (DE-Tha) and Braschaat (BE-Bra). Large symbols indicate location of the study sites and small symbols indicate the locations of the 20 closest sites from a European network (Babst *et al.*, 2013) used for comparison with tree-ring width (TRW) chronologies developed at the five study sites (Supporting Information Fig. S2).

multiple monoculture patches of different species and our sampling focused on Scots pine stands in the immediate vicinity of the flux tower. More detailed site descriptions are provided in Table 1.

All sites are located in relatively even-aged plantations with documented management (i.e. timber harvest) histories. Relevant thinning events occurred during the flux tower period in FI-Hyy (2001; Ilvesniemi *et al.*, 2009), DK-Sor (2007; Wu *et al.*, 2013), DE-Tha (2002; Grünwald & Bernhofer, 2007) and BE-Bra (1999; Gielen *et al.*, 2011). Understorey vegetation is generally very scarce as a result of local forest management practices, and the canopy-forming trees therefore contain the vast majority of the above-ground biomass. In addition, the footprint area of the CO₂ flux measurements can approximately be estimated from the principal wind direction and atmospheric stability, thus allowing comparable biometric forest growth data to be collected. Together, these five study sites span the principal European climate zones – boreal, temperate and Mediterranean – and, except for oak, represent the major European tree species.

Conceptual framework

Carbon assimilated by trees during photosynthesis is allocated to a variety of short- to long-term pools which together determine the carbon balance of a forest (Dixon *et al.*, 1994). In this study, we use tree-ring and biometric data to estimate the total above-ground woody carbon stocks (including stems, branches and bark biomass) to enable comparisons with eddy-flux measurements (Fig. 2). We thereby disregard other organs, such as foliage, fruits, coarse and fine roots, which are challenging to reliably assess over longer time-scales from *in situ* measurements and – in the case of foliage – may be temporally decoupled from wood formation through needle persistence or carbon storage legacies (Beck *et al.*, 2011; Richardson *et al.*, 2013). Biometric data are combined with the inter-annual growth variability from TRW measurements to reconstruct historical tree dimensions and transformed into tree-level estimates of the above-ground woody biomass increment (AWI) using allometric equations (Table 2). AWI was corrected for variability in XD, and then upscaled to the site level – a procedure facilitated by a fixed-plot sampling scheme (Babst *et al.*, 2012b). The annually resolved estimates of the total above-ground woody biomass increment (tAWI) served as a basis for comparison with EC data. We derived TER from NEP measurements and combined the two parameters into estimates of GPP. Periodical sums of all eddy fluxes were compiled to facilitate comparisons with tAWI.

Sample collection and biomass estimates

We applied a carbon-oriented sampling scheme at each study site designed to facilitate the reconstruction of tAWI from radial tree growth measurements (for a detailed description, see Babst *et al.*, 2012b). This approach involves the collection of tree-ring and biometric data (i.e. diameter at breast height (DBH) and tree height) from all trees within one or multiple predefined circular plots located in the footprint area of the respective flux tower. Plot number and size were adjusted according to the forest

Table 1 Description of study sites (climate data derived from the flux towers)

Site	Plots (radius (m))	Sp.1 (%)	Sp.2 (%)	No. of trees	TRW and XD chronos	Flux tower period	Annual mean T (°C)	Annual precip. (mm)	References
FI-Hyy	2 (10, 12.5)	<i>Pinus sylvestris</i> (> 95)	–	100	1969–2009	1996–2009	4.4	511	Rannik <i>et al.</i> (2002)
DK-Sor	1 (20)	<i>Fagus sylvatica</i> (> 95)	–	41	1925–2009	1996–2009	8.6	709	Pilegaard <i>et al.</i> (2011)
IT-SRo	2 (15, 15)	<i>Pinus pinaster</i> (87)	<i>Pinus pinea</i> (13)	97	1952–2009	1999–2009	15.3	859	Chiesi <i>et al.</i> (2005)
DE-Tha	2 (20, 20)	<i>Picea abies</i> (81)	<i>Larix decidua</i>	82	1899–2009	1996–2009	8.6	856	Grünwald & Bernhofer (2007)
BE-Bra	1 (22.5)	<i>Pinus sylvestris</i> (> 95)	–	48	1928–2009	1997–2009	11.1	860	Carrara <i>et al.</i> (2003)

TRW, tree-ring width; XD, average ring density.

composition to include a sufficient number of trees for exact dating (minimum of 40–50 individuals per plot; Fritts, 1976) and to capture a reasonably representative subset of the tower footprint. From all trees, we measured TRW, as well as earlywood and latewood width (EWW, LWW) and density (EXD, LXD), using a Walesch 2003 X-ray densitometer with a resolution of 0.01 mm. Brightness variations in the X-ray images were transferred into wood density using a standard calibration and species-specific relationships between absolute and radiographic wood density (Eschbach *et al.*, 1995). We calculated XD as the mean of EXD and LXD weighted by EWW and LWW, respectively. To test the regional representativeness of the annual growth anomalies from the study sites, we calculated standardized site chronologies for TRW and XD using a spline with a 50% frequency cutoff response at 30 yr (removing the biological age trend and most of the multi-decadal to centennial growth variability, Fritts, 1976; Esper *et al.*, 2002), and compared them with the 20 most proximal sites extracted from a European tree-ring network (Babst *et al.*, 2013).

Following the approach described in Babst *et al.* (2012b), we reconstructed historical tree diameters with the TRW starting

from the sampling year DBH (complete outermost 2009 ring) and assuming a linear relationship between wood and bark formation (Bakker, 2005). The annually resolved diameter reconstructions of each tree were transformed into AWI using multiple allometric biomass functions (Table 2) to permit some assessment of uncertainties in carbon stock estimates. We selected appropriate functions based on geographical proximity and valid diameter ranges. Consequently, the more widely studied species with numerous allometric functions ended up with a greater spread, but theoretically more robust mean estimates, than species with fewer available functions (i.e. Maritime pine in IT-SRo). We considered the prediction errors in AWI related to the use of allometric functions. As functions have different shapes and are often not published with sufficient fitting statistics to assess error propagation (e.g. as proposed by Nickless *et al.*, 2011), we implemented a simplified model of prediction error variance. Assuming the heteroscedastic nature of the biomass model residuals (Parresol, 1999), the variance of the prediction error is typically a power function of the independent variable (here DBH). We thus used the universal scaling exponent (2.3679) presented by Zianis & Menuccini (2004) to estimate the prediction error in AWI (irrespective of the species and biomass model used) as $\text{var}(\text{error}) = \text{DBH}^{2.3679}$. The 95% confidence interval around tAWI was estimated after summing all tree-level errors as $\pm 1.96 \times \text{sum}(\text{var}(\text{error}))^{0.5}$. This approach overestimated the prediction error by 10% compared with a function in which we were able to calculate the error based on the published statistics (Wutzler *et al.*, 2008), but underestimated errors compared with another approach (Zianis, 2008).

We refrained from combining our XD measurements with allometric volume functions to estimate tree biomass in this study, as: suitable volume equations were only available for the commercially relevant components (i.e. stem) of most species (Zianis *et al.*, 2005); and we were unable to collect wood density data from branches. Instead, we used the XD data to correct the AWI estimates for density variations within and between trees, and thereby to test questionable assumptions for a constant wood density in all allometric biomass functions (Supporting Information Fig. S1). This was achieved in two steps: correction for inter-annual XD variability (AWI multiplied by the XD anomaly in the respective year); and correction for the mean XD of a tree compared with the mean XD of all trees at a site.

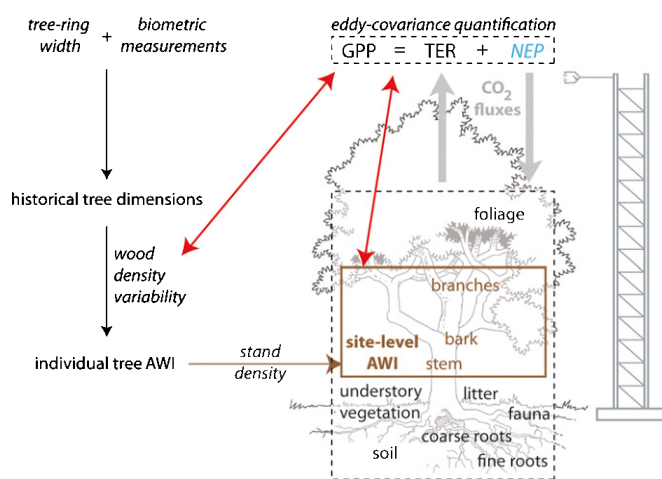


Fig. 2 Conceptual framework of this study with red arrows marking the principal assessments made. Field measurements are indicated in italic text (eddy-covariance in blue) and brown colors show the forest carbon pools (i.e. above-ground woody biomass increment, AWI) quantified using a combination of tree-ring and biometric data. Eddy-covariance parameters include gross primary productivity (GPP), terrestrial ecosystem respiration (TER) and net ecosystem productivity (NEP).

Table 2 Allometric biomass functions

Species	Input (DBH, height)	Biomass function (kg)	Reference
<i>Pinus sylvestris</i>	cm, –	$B = (10^{(0.981 + 2.289 \cdot \log_{10}(\pi \cdot \text{diameter}))}) / 1000$	Brakke (1996)
	cm, –	$B = 18.779 - 4.328 \cdot \text{diameter} + 0.506 \cdot (\text{diameter}^2)$	Briggs & Cunia (1982)
	cm, –	$B = \exp(-3.2807 + 2.6931 \cdot \log(\text{diameter}))$	Mäkelä & Vanninen (1998)
	cm, –	$B = \exp(-1.954 + 1.988 \cdot \log(\text{diameter}))$	Oleksyn <i>et al.</i> (1999)
	cm, –	$B_{\text{stem}} = 0.1227 \cdot \text{diameter}^2 \cdot 3.272$ $B_{\text{branches}} = 0.0022 \cdot \text{diameter}^2 \cdot 9.123$	Yuste <i>et al.</i> (2005)
<i>Fagus sylvatica</i>	cm, –	$B = 0.0798 \cdot \text{diameter}^2 \cdot 6.01$	Bartelink (1997)
	cm, –	$B = (10^{(2.85102 + 2.0666 \cdot \log_{10}(\text{diameter}))}) / 1000$	Duvigneaud & Timperman (1977)
	cm, –	$B = 0.1143 \cdot \text{diameter}^2 \cdot 5.03$	Pretzsch (2000)
<i>Picea abies</i>	cm, m	$B = 0.0523 \cdot \text{diameter}^2 \cdot 12 \cdot \text{height}^{0.655}$	Wutzler <i>et al.</i> (2008)
	cm, –	$B = 0.57669 \cdot \text{diameter}^{1.964}$	Cerny (1990)
<i>Pinus pinaster</i>	cm, –	$B = (10^{(1.81298 + 2.51353 \cdot \log_{10}(\text{diameter}))}) / 1000$	Duvigneaud & Timperman (1977)
	cm, –	$B = -43.13 + 2.25 \cdot \text{diameter} + 0.452 \cdot \text{diameter}^2$	Fiedler (1986)
	cm, –	$B = -60.55702 + 5.46558 \cdot \text{diameter} + 0.27567 \cdot \text{diameter}^2$	Pöppel (1989)
<i>Pinus pinaster</i>	cm, m	$B_{\text{stem}} = 6.3157 \cdot 10^{(-1)} + 1.584 \cdot 10^{(-2)} \cdot (\text{diameter}^2 \cdot \text{height})$ $B_{\text{branches}} = 1.25 + 4.7109 \cdot 10^{(-3)} \cdot (\text{diameter}^2 \cdot \text{height})$	Tabacchi <i>et al.</i> (2011)

DBH, diameter at breast height.

We calculated tAWI as the summed AWI of all individual trees divided by the total sampling area (Table 1). To quantify the annual carbon allocation to stems and branches, we assumed 50% carbon content in woody tissues (Joosten *et al.*, 2004), unless site-specific estimates were available (e.g. DK-Sor: 46% and 47% in stems and branches, respectively). Validation of tAWI was performed when site-specific biometric estimates of above-ground woody biomass increment were available. At the FI-Hyy site, validation followed the approach presented by Repola (2009) with historical tree heights reconstructed according to Ilvesniemi *et al.* (2009). In DK-Sor, estimates of carbon uptake based on novel biomass expansion functions (Skovsgaard & Nord-Larsen, 2012) and corrected for management influences were used for evaluation. In BE-Bra, tAWI was tested against annual changes in above-ground wood production based on site-specific allometric relationships (Yuste *et al.*, 2005).

Eddy-covariance (EC) measurements

The EC technique (Aubinet *et al.*, 2012), together with a number of relevant meteorological variables (radiation, temperature, precipitation), measures the energy, carbon and water fluxes between ecosystems and the atmosphere. Over the last 15 yr, a European network of sites has been established with long-term measurements available from the European Fluxes database (www.europe-fluxdata.eu). All EC data used in this study were processed and quality controlled according to the standard methodology described by Papale *et al.* (2006), and gapfilled to allow the calculation of annual budgets using the methodology described in Reichstein *et al.* (2005). The friction velocity (u^*) thresholds at each site were calculated annually to allow adjustment for changes in the roughness, for example, as a result of canopy evolution, disturbances or changes in the site setup, but tests in FI-Hyy showed that annual NEP was rather insensitive to the choice of annual vs fixed u^* thresholds (D. Papale *et al.*, unpublished). A detailed propagation of uncertainty associated with u^* calculation

at each site, however, is outside the scope of this article. Parameters used in our analyses include monthly NEP and its components GPP and TER. To partition NEP into TER and GPP, TER was estimated by extrapolating night-time measurements to daytime using short-term temperature sensitivity relations (Reichstein *et al.*, 2005). This approach has been shown to yield inter-annual variability which is comparable with other partitioning methods (Desai *et al.*, 2008), and the magnitude of the GPP obtained is similar to that obtained from a daytime extrapolation approach (Lasslop *et al.*, 2010). No data for 2003 are available at the BE-Bra site (Gielen *et al.*, 2011). Correlation and linear regression analyses between biometric (tAWI and XD) and EC measurements were performed at monthly, seasonal and annual time-scales. In addition, we assessed the fraction of sequestered carbon which is allocated to above-ground wood formation to support different growth processes related to volume and wood density increase.

Results

Inter-annual growth variability

We measured a total of 384 TRW and XD time series from five flux tower sites (common period 1970–2009) to quantify the magnitude and inter-annual variability in tree growth (Fig. 3, left panels). Decadal trends in radial increments were observed at the FI-Hyy and IT-SRo sites, largely related to the geometric age trend and juvenile growth effects. Other sites showed no longer term trends or abrupt discontinuities (e.g. caused by forest management events or severe climate extremes) during the past 40 yr. Generally, mean correlations of the TRW and XD time series among trees at a site are higher than $r = 0.3–0.4$ ($P < 0.05$). Correlations at the FI-Hyy and IT-SRo sites are even higher (up to $r = 0.8$, $P < 0.001$) as a result of common age-related trends, and decline to $r = 0.29$ ($P = 0.047$) and $r = 0.48$ ($P = 0.009$) after de-trending. To test whether growth variability observed at our

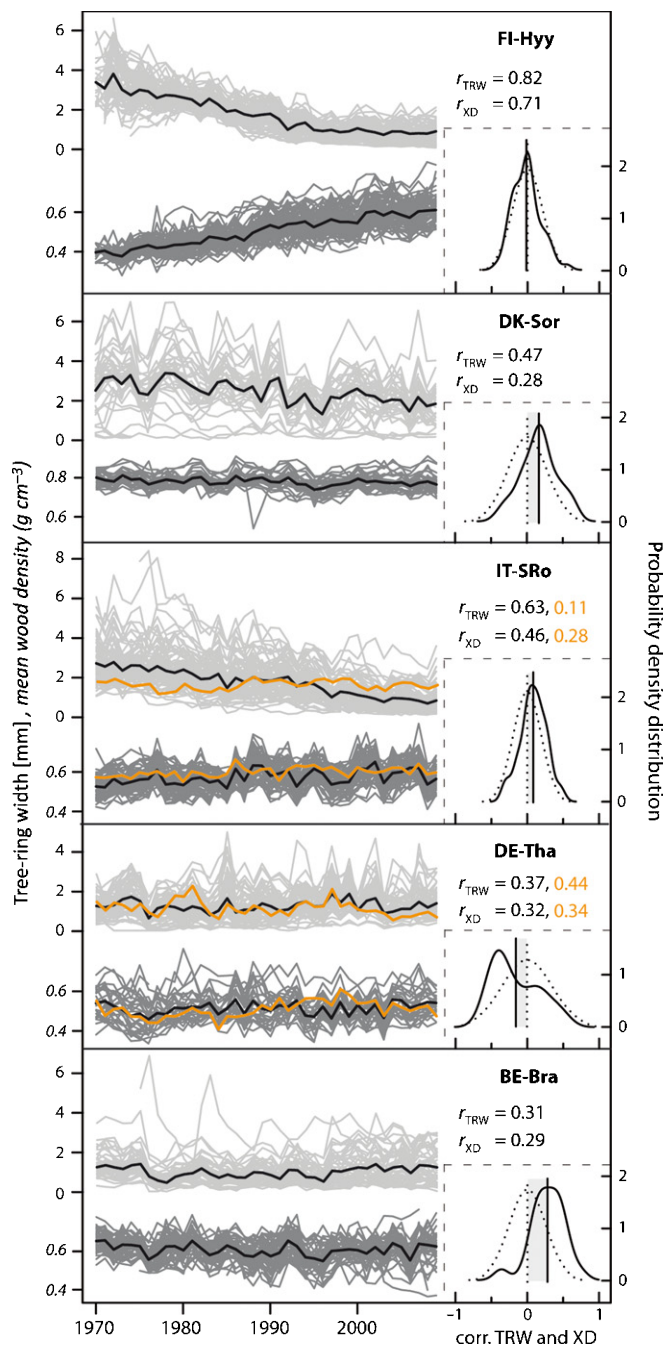


Fig. 3 Left panels show the raw tree-ring width (TRW, light gray) and mean wood density (XD, dark gray) series measured at the five study sites. Mean chronologies are shown in black for primary and in orange for secondary species (if present). Average inter-series correlations are displayed in the respective colors (critical value for significant correlations is $r = 0.264$ at $P = 0.05$). Right panels show the probability density functions of the tree-level correlations between TRW and XD (solid lines). Significant ($P < 0.1$) differences between observed (solid) and target normal (dotted) distributions are shaded in gray.

study sites is representative at regional scales, we compared the de-trended site chronologies (only TRW as XD measurements are rarely available) with the 20 spatially closest sites from a European tree-ring network (Fig. S2). For all sites except IT-SRo, TRW indices correlate significantly ($r = 0.35$, $P = 0.043$ to

$r = 0.75$, $P < 0.001$) with the mean of the surrounding chronologies, thus suggesting regionally coherent inter-annual variations in above-ground biomass increment. In addition, we found common negative growth anomalies among our study sites which correspond to known large-scale climate anomalies (Babst *et al.*, 2012a) in the years 2006 (DK-Sor, BE-Bra), 2003 (FI-Hyy, IT-SRo, DE-Tha), 1996 (DK-Sor, BE-Bra), 1992 (FI-Hyy, DK-Sor) and 1976 (DK-Sor, DE-Tha, BE-Bra), where no management interventions took place.

Variability in TRW and XD often follows unique climatic drivers (Briffa *et al.*, 2002; Frank & Esper, 2005), with the effect that annual ring width and density may exert opposing (but also amplifying) influences on AWI. To assess the systematic relationships between both parameters, we tested the probability density functions (PDFs) of the tree-level correlations between de-trended TRW and XD: (1) for normality (Shapiro–Wilk test); and (2) for significant differences from target normal distributions (equal standard deviation and a mean of zero; Student's *t*-test). As shown in Fig. 3 (right panels), distributions were significantly shifted towards positive correlations in DK-Sor ($r = 0.16$, $P = 0.01$), IT-SRo ($r = 0.13$, $P = 0.004$) and BE-Bra ($r = 0.28$, $P < 0.001$), and towards negative correlations in DE-Tha ($r \sim -0.15$, $P = 0.05$). No significant relationship between TRW and XD was observed at the FI-Hyy site ($r = -0.01$, $P = 0.75$). Depending on their sign, differences between the observed PDFs and null distributions indicate XD variations which either amplify (positive correlation) or buffer (negative correlation) AWI fluctuations inferred from TRW alone. At the site level, positive correlations between TRW and XD were found in IT-SRo and BE-Bra ($r = 0.3$, $P = 0.05$ and $r = 0.52$, $P < 0.001$, respectively), whereas relationships were not significant at other sites.

Carbon uptake

We quantified carbon uptake with both biometric and EC approaches during the 1997–2009 period commonly covered by flux tower and tree-ring time series. Estimates of XD-corrected tAWI (Fig. 4a) indicate that, during this time, mean carbon allocation rates to above-ground woody tissues were highest at the IT-SRo site ($370 \pm 50 \text{ g C m}^{-2} \text{ yr}^{-1}$), followed by DK-Sor ($300 \pm 50 \text{ g C m}^{-2} \text{ yr}^{-1}$), DE-Tha ($150 \pm 60 \text{ g C m}^{-2} \text{ yr}^{-1}$), BE-Bra ($130 \pm 50 \text{ g C m}^{-2} \text{ yr}^{-1}$) and FI-Hyy ($110 \pm 100 \text{ g C m}^{-2} \text{ yr}^{-1}$). Over the investigated time, tAWI increased considerably at the DK-Sor and moderately at the FI-Hyy and BE-Bra sites. By contrast, IT-SRo and DE-Tha showed a decline in woody carbon uptake. Site-specific reference datasets (based on Repola, 2009 – FI-Hyy; Skovsgaard & Nord-Larsen, 2012 – DK-Sor; Yuste *et al.*, 2005 – BE-Bra) used to evaluate tAWI estimates show similar inter-annual variability, and are mostly within the uncertainty range derived from the allometric equations, but indicate 20% higher mean allocation rates at FI-Hyy, and 16% and 5% lower rates at DK-Sor and BE-Bra, respectively (Fig. 4a). Our results indicate that the more productive sites show a higher inter-annual variability in tAWI. A significant positive relationship ($r^2 = 0.86$, $P = 0.02$) was found between mean tAWI among

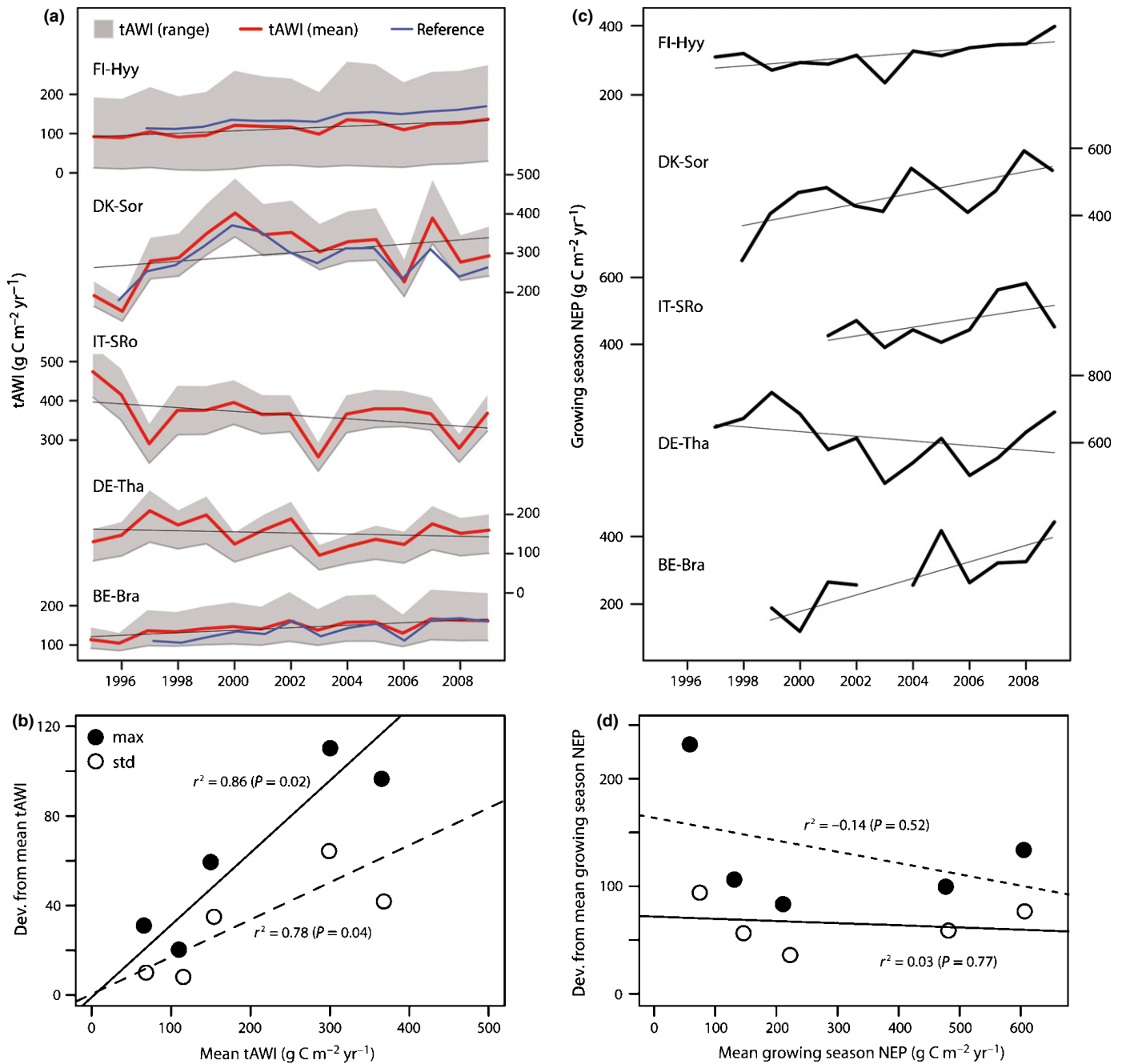


Fig. 4 Inter-annual variability of (a) tree-ring-derived total above-ground woody biomass increment (tAWI) and (c) eddy-covariance-based net ecosystem productivity (NEP) measurements. Uncertainty ranges around tAWI result from multiple biomass functions and their estimated residual errors (means shown in red) and site-specific reference data are shown in blue (where available). In addition, the relationships between (b) mean tAWI and (d) mean NEP with the respective standard (open circles) and maximum (closed circles) deviations during the flux tower period are presented.

sites and their standard and maximum deviations (Fig. 4b). Comparison of the XD-corrected and uncorrected tAWI estimates was performed to quantify potential biases introduced by the assumption of a constant wood density in allometric biomass equations (Wirth *et al.*, 2004; Wutzler *et al.*, 2008). Although the mean XD of trees at each site is highly variable (Fig. S1), the average effect of our XD correction on tAWI was $< 5\%$ at all sites except FI-Hyy, where the uncorrected tAWI was $\approx 20\%$ lower. At inter-annual time-scales, however, differences between XD-corrected

and uncorrected tAWI of up to $\approx 10\%$ were observed at all sites (Fig. S3).

Figure 4(c) shows the total ecosystem carbon uptake (NEP) during the growing season, which was defined as starting in the month when GPP first increases (Fig. S4; see Fig. S5 for annual fluxes) and ending in September when tree-ring formation probably approaches completion in the investigated climate regimes (Moser *et al.*, 2010). Mean growing season NEP over the flux tower period was highest in DE-Tha ($616 \text{ g C m}^{-2} \text{yr}^{-1}$),

followed by IT-SRo (464 g C m⁻² yr⁻¹), DK-Sor (459 g C m⁻² yr⁻¹), FI-Hyy (315 g C m⁻² yr⁻¹) and BE-Bra (259 g C m⁻² yr⁻¹). This order mirrors that found in tAWI, except for the DE-Tha site. Similarly, trends observed in NEP at the five study sites reflect the tAWI results, except in IT-SRo, where the EC data indicate an increase in ecosystem productivity, whereas tAWI decreases. In contrast with the biometric observations, no significant relationship between the magnitude and inter-annual variability of NEP was found (Fig. 4d).

Correlation between wood production and carbon fluxes

The inter-annual variability in de-trended tAWI and XD was compared with the monthly and seasonal aggregates of CO₂ fluxes (i.e. NEP and GPP) to investigate the seasonality of carbon allocation to above-ground woody tissues. We calculated Pearson's correlation coefficients between de-trended tree-ring and EC measurements for all possible combinations of months between January and September (Fig. 5), and tested the significance ($P < 0.05$, two-tailed) of the relationships obtained after applying a Bonferroni correction to the P values (Hochberg, 1988). Critical correlation values (Table S1) were determined with the test number adjusted to the number of months included in the respective seasons. Results differ between the study sites and the observed patterns were stronger for NEP than for GPP at four out of the five sites (except BE-Bra). In FI-Hyy, the highest correlations between tAWI and NEP emerged in early summer (i.e. January to May and June; $r = 0.75$, $P = 0.02$ and $r = 0.66$, $P = 0.05$, respectively) and in August ($r = 0.73$, $P = 0.02$). For XD, the August–September ($r = 0.62$, $P = 0.07$) as well as February ($r = 0.73$, $P = 0.02$) signals were strongest. In DK-Sor, correlations between tAWI and NEP were generally weak (January–June, $r = 0.5$, $P = 0.24$). Relationships with XD were stronger and peaked over the January–June season ($r = 0.7$, $P = 0.03$). At the It-SRo site, June–July NEP showed highest agreement with tAWI ($r = 0.81$, $P = 0.006$), whereas a weak XD signal peaked in June ($r = 0.64$, $P = 0.06$). In DE-Tha, pronounced early spring and summer signals were observed for tAWI (January–June, $r = 0.72$, $P = 0.02$), whereas correlations in the in-between season (i.e. May) were lower. For XD, the strongest match with late-summer (i.e. August) NEP and GPP was found ($r = 0.61$, $P = 0.09$ and $r = 0.77$, $P = 0.01$, respectively). At the BE-Bra site, signals were generally weak and below significance for tAWI and XD. A similar analysis comparing tAWI and XD with the previous year's (i.e. pApril–pDecember) fluxes revealed inconsistent patterns (Fig. S6). Significant correlations were observed in FI-Hyy between tAWI and pDecember GPP ($r = -0.78$, $P = 0.01$), in IT-SRo between tAWI and pNovember–pDecember NEP ($r = -0.71$, $P = 0.03$) and in BE-Bra between XD and pAugust and pSeptember–pOctober NEP ($r = 0.76$, $P = 0.01$ and $r = 0.68$, $P = 0.04$, respectively).

From this extensive analysis, two seasons emerged with consistently good agreement between tree-ring measurements and NEP among all sites, namely: (1) between tAWI and NEP during the early growing season (January to June/July; Fig. 6a); and (2) XD and NEP towards the end of the growing season

(August–September; Fig. 6b). These signals are influenced by forest management practices and tend to be weaker when years before the last thinning event are included. Accordingly, the observed correlation between NEP and tAWI at the FI-Hyy site ($r = 0.66$, $P = 0.05$ between 2001–2009) is no longer statistically significant (Table S1) if the pre-thinning period 1997–2000 (Ilvesniemi *et al.*, 2009) is considered. Thinning events in DK-Sor (2007; Wu *et al.*, 2013) and DE-Tha (2002; Grünwald *et al.*, 2007) had less influence on the agreement between tAWI and NEP.

Woody carbon sequestration vs ecosystem carbon fluxes

The fraction of NEP, GPP and TER associated with tAWI was assessed in an attempt to better constrain carbon allocation to above-ground woody biomass during the main growing season (Fig. 7). Uncertainty around the tAWI to flux ratios originates from the inter-annual variability in both data streams and from the multiple allometric models considered in tAWI estimates. At the most productive sites (i.e. DK-Sor and IT-SRo), tAWI explained up to 80% of NEP, 20–25% of GPP and 23–32% of TER. In FI-Hyy and BE-Bra, the two least productive sites, 32–38% of NEP, 10–12% of GPP and 15–18% of TER were associated with above-ground woody biomass increment. In DE-Tha, tAWI accounted for 25% of NEP, 13% of GPP and 17% of TER. In addition, we calculated the respective correlation coefficients between tAWI and growing season EC measurements to investigate the explanatory power of tree-ring data with regard to inter-annual variability compared with absolute carbon uptake (Fig. 7). This comparison revealed somewhat opposite results for NEP and GPP. tAWI appears to be a better measure of the inter-annual variability of GPP than would be expected from its absolute fraction of GPP at all study sites. With regard to NEP, however, the fraction of total carbon uptake explained by tAWI is considerably higher than the inter-annual variability at the FI-Hyy, DK-Sor and IT-SRo sites. In DE-Tha, the opposite result was obtained, whereas the explanatory power of tAWI for the magnitude and dynamics of forest carbon uptake was comparable at the BE-Bra site.

Discussion

This study quantified carbon sequestration in tree stems and branches at five European flux tower sites using a combination of extensive tree-ring and biometric measurements, and linked these measurements with long-term EC datasets aiming to better constrain carbon allocation to above-ground woody tissues. In line with results from earlier studies (Curtis *et al.*, 2002; Peichl *et al.*, 2010), we observed large variation in the NEP fraction explained by tAWI from year to year. The variability tended to be larger at sites with lower mean tAWI to NEP ratios. By contrast, the fraction of GPP used for wood production is small and the tAWI to GPP ratios observed at our study sites (Fig. 7) are within the range reported in a recent global investigation (Vicca *et al.*, 2012). Seasonal relationships between biomass increment and GPP were weaker than with NEP, which indicates that most of

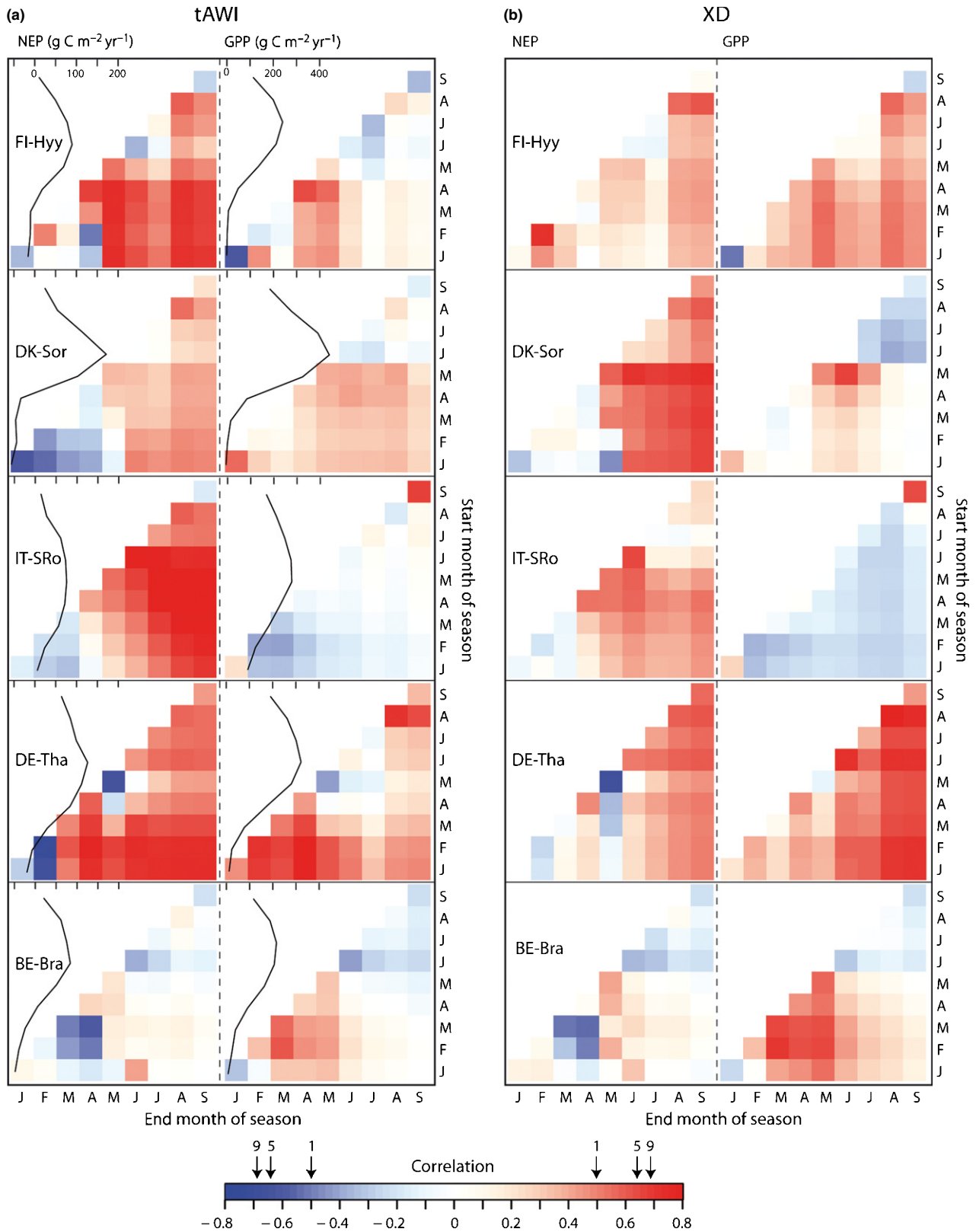


Fig. 5 Relationships between (a) total above-ground woody biomass increment (tAWI) and (b) mean wood density (XD) with net ecosystem productivity (NEP) and gross primary production (GPP) during all possible combinations of months over the January–September period. Correlations for individual months are shown on the diagonals (e.g. bottom line 1st = January), whereas seasons extend to the right (e.g. bottom line 2nd = January–February, 3rd = January–March, etc.). In addition, the seasonal courses of NEP and GPP are shown in (a) as indicators of the growing seasons at the respective sites. Arrows above the correlation legend mark the critical values (after a Bonferroni correction to the *P* values) for significant correlations over season lengths of 1, 5 and 9 months. Critical values for other season lengths are provided in Table S1.

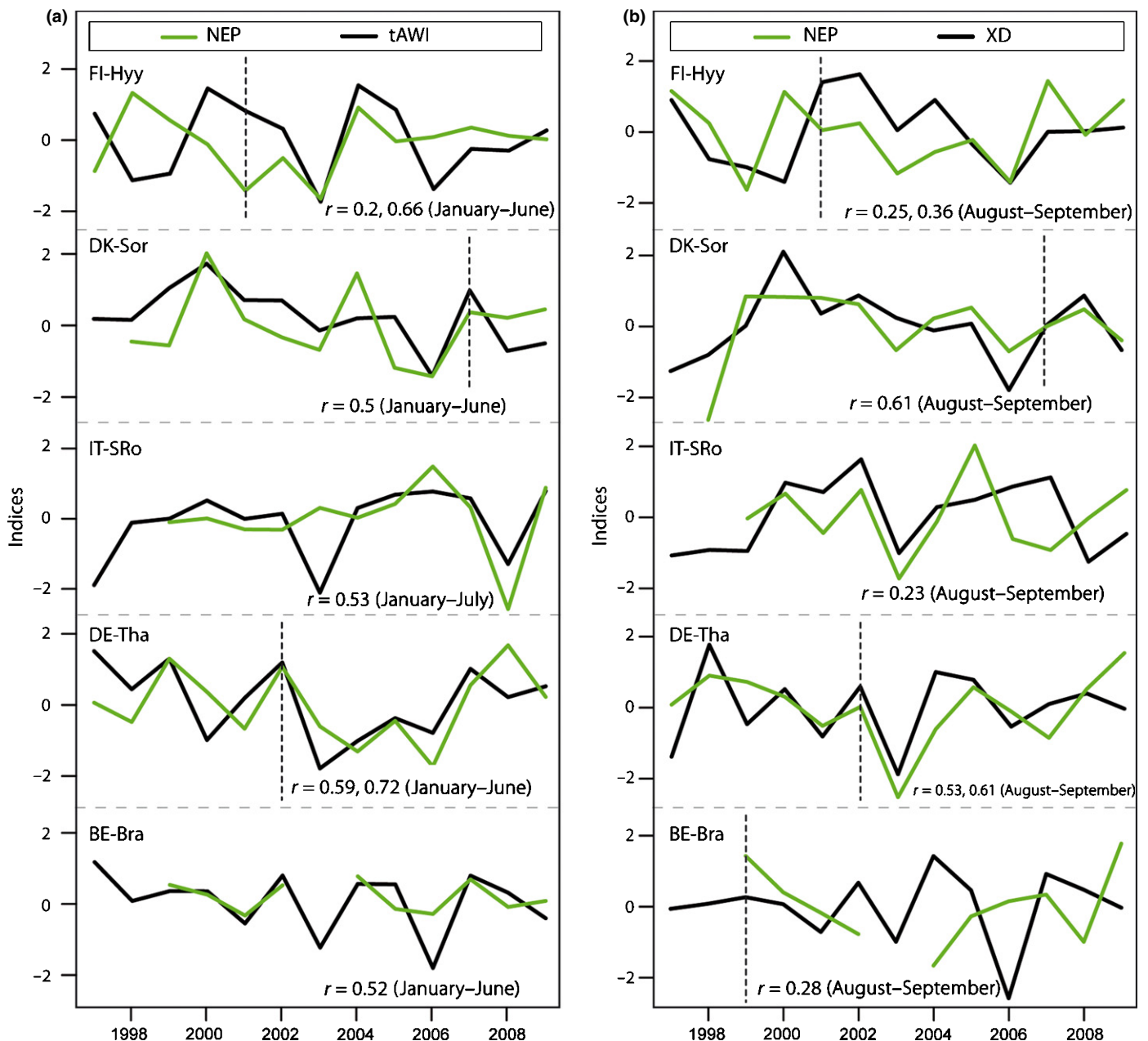


Fig. 6 Inter-annual variability in de-trended (a) total above-ground woody biomass increment (tAWI) and early season net ecosystem productivity (NEP), and (b) mean wood density (XD) and late season NEP (seasons indicated in parentheses). Vertical dashed lines mark forest management interventions (i.e. thinning) at the respective sites, and correlation coefficients are presented for the entire and the post-thinning period (see Table S1 for r_{crit}).

NEP goes to wood production, not to other biomass pools or soils (Vicca *et al.*, 2012). However, the relationship between NEP and tAWI was strongest at our sites if at least one growing season month in which NEP is mostly GPP driven was considered. This finding, together with the modest TER fraction and variability represented by tAWI, points to a strong influence of GPP on tAWI. The common sensitivity of assimilation and radial growth to the water balance (Beer *et al.*, 2007) may serve as an explanation here. NEP, however, is driven by a complex set of processes, including more temperature-sensitive mechanisms (i.e. TER; Reichstein *et al.*, 2005), which are not so closely coupled to radial tree growth. The observed relationships represent a step

towards resolving forest carbon dynamics using *in situ* measurements, and may also help to improve vegetation model parameterizations and hence decrease uncertainties in model projections of terrestrial carbon cycling (Keenan *et al.*, 2012).

The TRW and XD datasets produced herein provide insights into a wide span of ecological, competitive, climatic and management regimes (see references in Table 1). In addition, the XD measurements permitted us to quantify and mitigate biases introduced by the assumption of constant wood density in most allometric models (Zianis *et al.*, 2005; Wutzler *et al.*, 2008). This XD correction assumes similar inter-annual wood density variability in stem and branch wood, which was reported for Scots pine

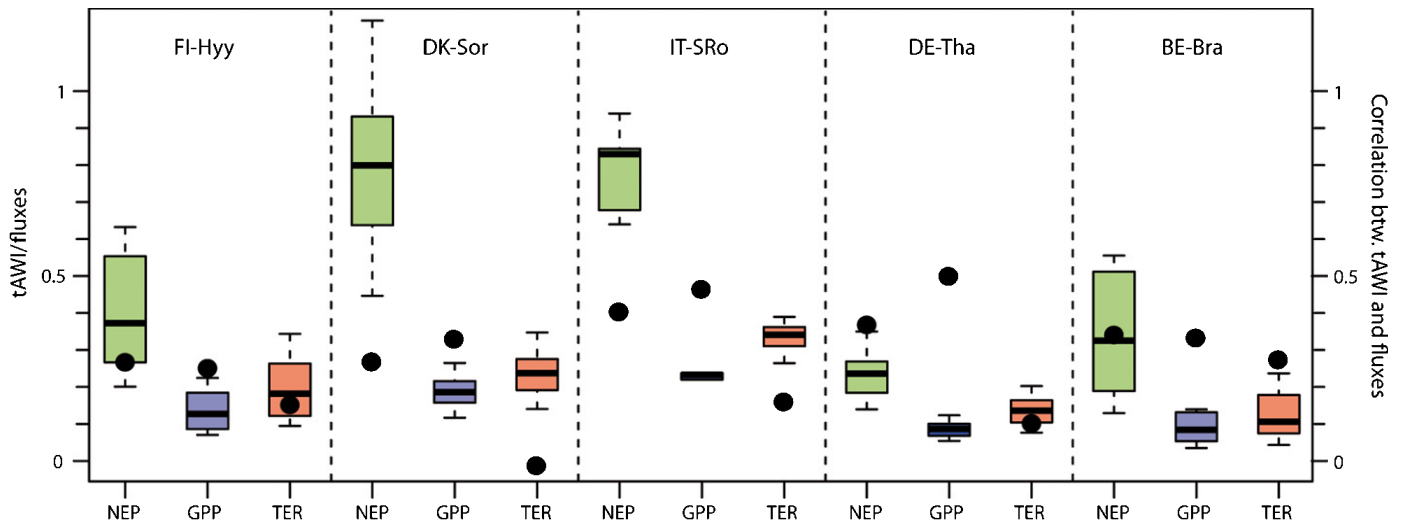


Fig. 7 Fractions of growing season net ecosystem productivity (NEP, green), gross primary productivity (GPP, blue) and terrestrial ecosystem respiration (TER, red) represented by total above-ground woody biomass increment (tAWI), thereby considering the inter-annual variability in CO₂ fluxes and woody carbon uptake derived from multiple biomass functions. Boxes represent the 25th to 75th percentiles (means indicated by horizontal bars) and whiskers show the full range. Black dots indicate correlations between the respective parameters over the time period covered by eddy-covariance measurements.

(Mäkinen, 1999), but lacks testing in many tree species and forest types. Relationships between TRW and XD differed between study sites, suggesting that biometric studies exclusively based on changes in tree diameter may provide a locally biased picture of the sensitivity and resilience of woody biomass production to climate variation and extremes. The effect of XD variability, however, is smaller than that of tAWI variability, and the sign of their correlation may reflect dependence on site properties (e.g. sparse vs dense stands in BE-Bra and FI-Hyy, respectively, both Scots pine), as well as on species-specific characteristics. These relationships will need to be tested with additional sites, species, forest types and climate zones to uncover more general patterns and to quantify their impact on estimations of forest growth, for example, based on dendrometer bands (Zweifel *et al.*, 2010).

The direct comparison between tAWI and EC was challenged by five principal factors which we will address. (1) tAWI is mainly related to biomass increment, whereas EC data are an integral measurement of physiological processes related to carbon assimilation, allocation and use (Baldocchi, 2003). Earlier studies have shown that stem growth alone is an insufficient proxy for total biomass production (Mund *et al.*, 2010). Consequently, the relationship between tAWI and NEP is expected to be weakened by carbon allocation dynamics to other storage pools (Brüggemann *et al.*, 2011), by potential changes in growth dynamics along the stem (Bouriaud *et al.*, 2005) and by the heterotrophic respiration component of NEP – factors which all respond to different environmental drivers. These dynamics further involve temporally lagged processes, with a considerable fraction of the annual stem growth affected by the previous growing season (Skomarkova *et al.*, 2006), thus leading to a strong control of stored carbon on spring fluxes (Kuptz *et al.*, 2011). (2) Uncertainty may be introduced by the spatial and seasonal (in-)compatibility of tree-ring and EC datasets. As the footprint area varies in time, size and location as a result of

weather conditions (Chen *et al.*, 2009), the sampling plots may be more or less representative of the EC fluxes. Without fully sampling all trees within the footprint area, some errors caused by spatial variations in species composition, stem distribution and competition will always exist in sampling approaches. However, multiple sampling plots at individual sites provided similar tAWI estimates (Babst *et al.*, 2012b), suggesting that the forest structure is rather homogeneous and is captured reasonably well by our approach. (3) The applicability of the biometric functions for our specific sites could not be considered in this study because functions are often not published with sufficient detail. Our estimates of residual error propagation are thus not function specific and the uncertainty ranges around the mean tAWI may in reality be different from those shown in Fig. 4. Validation against individual functions indicated either an overestimation (Wutzler *et al.*, 2008) or an underestimation (Zianis, 2008) of the residual errors. (4) Management practices may exhibit strong impacts on both EC fluxes (Etzold *et al.*, 2011) and the growth performance of remaining trees (Skomarkova *et al.*, 2006). Consequently, NEP and tAWI may be partly decoupled before the last thinning events, as the flux measurements include signals from trees not present in the sampling year and thinning also alters the growth physiology (e.g. may reduce competition and accentuate climatic growth limitations). As evidenced in Fig. 6, relationships may thus be considerably stronger in the most recent period. (5) Importantly, the short time periods (9–13 yr) assessed through EC measurements result in few degrees of freedom to obtain statistically significant correlations (Table S1). Although our comparisons between biometric and EC-based carbon sink estimates provide comprehensive and mechanistically straightforward seasonal links, the inferred relationships should be revisited at these sites as EC records become longer and tested at independent locations.

Despite the above challenges, we found reasonably strong seasonal agreement between biometric measurements and NEP at most study sites. Comparisons of these results with existing studies are challenging because of inconsistent approaches for the assessment of radial tree growth and because of the different bioclimatic zones investigated (Curtis *et al.*, 2002; Rocha *et al.*, 2006; Gough *et al.*, 2008; Granier *et al.*, 2008; Ilvesniemi *et al.*, 2009; Ohtsuka *et al.*, 2009; Zweifel *et al.*, 2010; Gielen *et al.*, 2013). Our findings indicate a strong relationship among study sites between tAWI and NEP during the January to June/July season, where most of the radial growth is realized and soil water reserves are high. This result is consistent with earlier studies reporting robust links between radial growth and spring to early summer EC measurements (Granier *et al.*, 2008). In addition, we observed reasonably high positive correlations between XD and late summer (i.e. August–September) NEP at three of the five sites. This seasonal partitioning in carbon allocation: (1) points towards a specific timing of wood production and carbon assimilation as photosynthesis continues after radial growth has stopped; (2) is mechanistically straightforward in terms of cell formation and maturation processes (Moser *et al.*, 2010); and (3) suggests that carbon sequestered after June/July is mostly used for cell wall thickening processes (i.e. XD increase; Lupi *et al.*, 2012) and/or stored in above- and below-ground nonstructural carbohydrate reserves (Granier *et al.*, 2008; Wolf *et al.*, 2011; Richardson *et al.*, 2013). The latter fraction can be rather large and is known to support next year's spring growth (Skomarkova *et al.*, 2006) or used up to several years later (Richardson *et al.*, 2013). In the present study, relationships between tAWI and XD with the previous year's fluxes were not robust (Fig. S6), and the explicit quantification of carbon storage will require longer term assessments of all forest carbon pools and their differing turnover rates. Interestingly, the tAWI to NEP ratio was higher at the more productive sites, which also showed the strongest inter-annual variability in wood formation (Fig. 4). The forest carbon sink at these productive sites is thus probably most susceptible to extreme climatic events (Reichstein *et al.*, 2007, 2013).

Our synthesis of above-ground biomass increment from the most important European climate zones and tree species helps us to better understand seasonal carbon allocation processes, and demonstrates that variability in tree-ring and monthly to seasonal EC measurements are largely compatible and complementary. Yet, carbon allocation to above-ground woody tissues may be altered by climate warming with different impacts expected in boreal and temperate regions (Lindner *et al.*, 2010). For instance, warmer temperatures may enhance root and foliage growth in response to an earlier start of the growing season (Kallikokoski *et al.*, 2012; Lapenis *et al.*, 2013). In addition, the considerable inter-annual variations in above-ground biomass increment emphasize the relevance of, for example, extreme climatic events for the terrestrial carbon balance and the need for extensive *in situ* studies of climate–growth interactions. Our assessments provide a framework to link future biometric and EC measurements that will contribute to a better quantification of long-term changes in terrestrial carbon uptake and will reduce uncertainties for carbon cycle–climate feedbacks.

Acknowledgements

This work was funded by the CARBO-Extreme project (FP7-ENV-2008-1-226701) and the Swiss National Science Foundation (NCCR Climate). The authors would like to thank Anne Verstege and Fabienne Bauer for their efforts during fieldwork, as well as Daniel Nievergelt and Anne Verstege for their help with wood density measurements. We thank Jan Esper, Soumaya Belmecheri, Stefan Klesse, Valerie Trouet, Ross Alexander and Alicja Babst-Kostecka for fruitful discussions. In addition, we thank all the people involved in maintenance and measurement work at the EC stations. I.A.J. further acknowledges the Flemish Science Fund (FWO) for financial support.

References

- Amiro BD, Barr AG, Barr JG, Black TA, Bracho R, Brown M, Chen J, Clark KL, Davis KJ, Desai AR *et al.* 2010. Ecosystem carbon dioxide fluxes after disturbance in forests of North America. *Journal of Geophysical Research: Biogeosciences* 115: 1–13.
- Aubinet M, Vesala T, Papale D. 2012. *Eddy covariance – a practical guide to measurement and data analysis*. Heidelberg, Germany: Springer Atmospheric Sciences.
- Babst F, Bouriaud O, Frank DC. 2012b. A new sampling strategy for tree-ring based forest productivity estimates. *ATR TRACE Proceedings* 10: 62–70.
- Babst F, Carrer M, Poulter B, Urbinati M, Neuwirth B, Frank D. 2012a. 500 years of regional forest growth variability and links to climatic extreme events in Europe. *Environmental Research Letters* 7: 1–11.
- Babst F, Poulter B, Trouet V, Tan K, Neuwirth B, Wilson R, Carrer M, Grabner M, Tegel W, Levanić T *et al.* 2013. Site- and species-specific responses of forest growth to climate across the European continent. *Global Ecology and Biogeography* 22: 706–717.
- Bakker JD. 2005. A new, proportional method for reconstructing historical tree diameters. *Canadian Journal of Forest Research* 35: 2515–2520.
- Baldocchi D. 2003. Assessing the eddy-covariance technique for evaluating carbon dioxide exchange rates of ecosystems: past, present and future. *Global Change Biology* 9: 1–14.
- Barford CC, Wofsy SC, Goulden ML, Munger JW, Pyle EH, Urbanski SP, Hutyyra L, Saleska SR, Fitzjarrald D, Moore K. 2001. Factors controlling long- and short-term sequestration of atmospheric CO₂ in a mid-latitude forest. *Science* 294: 1688–1691.
- Bartelink H. 1997. Allometric relationship for biomass and leaf area of beech (*Fagus sylvatica* L.). *Annals of Forest Science* 54: 39–50.
- Beck P, Juday G, Alix C, Barber V, Winslow S, Sousa E, Heiser P, Herriges J, Goetz S. 2011. Changes in forest productivity across Alaska consistent with biome shift. *Ecology Letters* 14: 373–379.
- Beer C, Reichstein M, Ciais P, Farquhar GD, Papale D. 2007. Mean annual GPP of Europe derived from its water balance. *Geophysical Research Letters* 34: L05401.
- Bouriaud O, Breda N, Dupouey J, Granier A. 2005. Is ring width a reliable proxy for stem-biomass increment? A case study in European beech. *Canadian Journal of Forest Research* 35: 2920–2933.
- Bouriaud O, Breda N, Le Moguedec G, Nepveu G. 2004. Modelling variability of wood density in beech as affected by ring age, radial growth and climate. *Trees – Structure and Function* 18: 264–276.
- Brakke H. 1996. Distribution and yield of biomass from young *Pinus sylvestris* and *Picea abies* stands on drained and fertilized peatland. *Scandinavian Journal of Forest Research* 1: 49–66.
- Briffa K, Osborn T, Schweingruber F, Jones P, Shiyatov S, Vaganov E. 2002. Tree-ring width and density data around the Northern Hemisphere: part 1, local and regional climate signals. *The Holocene* 12: 737–757.
- Briggs E, Cunia T. 1982. Effect of cluster sampling in biomass tables construction: linear regression models. *Canadian Journal of Forest Research* 12: 255–263.

- Brüggemann N, Gessler A, Kayler Z, Keel SG, Badeck F, Barthel M, Boeckx P, Buchmann N, Brugnoli E, Esperschütz J *et al.* 2011. Carbon allocation and carbon isotope fluxes in the plant–soil–atmosphere continuum: a review. *Biogeosciences* 8: 3457–3489.
- Campioli M, Gielen B, Göckede M, Papale D, Bouriaud O, Granier A. 2011. Temporal variability of the NPP–GPP ratio at seasonal and interannual time scales in a temperate beech forest. *Biogeosciences* 8: 2481–2492.
- Carrara A, Kowalski A, Neiryck J, Janssens I, Curiel Y, Ceulemans R. 2003. Net ecosystem CO₂ exchange of mixed forest in Belgium over 5 years. *Agricultural and Forest Meteorology* 119: 209–227.
- Cerny M. 1990. Biomass of *Picea abies* (L.) Karst. in midwestern Bohemia. *Scandinavian Journal of Forest Research* 5: 83–95.
- Chen B, Black T, Coops N, Hilker T, Trofymow J, Morgenstern K. 2009. Assessing tower flux footprint climatology and scaling between remotely sensed and eddy covariance measurements. *Boundary-Layer Meteorology* 130: 137–167.
- Chiesi M, Maselli F, Bindi M, Fibbi L, Cherubini P, Arlotta E, Tirone G, Matteucci G, Seufert G *et al.* 2005. Modelling carbon budget of Mediterranean forests using ground and remote sensing measurements. *Agricultural and Forest Meteorology* 123: 22–34.
- Curtis P, Hanson P, Bolstad P, Barford C, Randolph J, Schmid H, Wilson K. 2002. Biometric and eddy-covariance based estimates of annual carbon storage in five eastern North American deciduous forests. *Agricultural and Forest Meteorology* 113: 3–19.
- Desai AR, Richardson AD, Moffat AM, Kattge J, Hollinger DY, Barr A, Falge E, Noormets A, Papale D, Reichstein M *et al.* 2008. Cross-site evaluation of eddy covariance GPP and RE decomposition techniques. *Agricultural and Forest Meteorology* 148: 821–838.
- Dixon R, Brown S, Houghton R, Solomon A, Trexler M, Wisniewski J. 1994. Carbon pools and flux of global forest ecosystems. *Science* 263: 185–191.
- Duvigneaud P, Timperman P. 1977. Biomasse des epiphytes cryptogamiques dans une hêtre ardennaise. In: Duvigneaud P, Kestemont P, eds. *Productivité biologique en Belgique*. Paris, France: Editions Duculot, 107–154.
- Eschbach W, Nogler P, Schär E, Schweingruber FH. 1995. Technical advances in the radiodensitometrical determination of wood density. *Dendrochronologia* 13: 155–168.
- Esper J, Cook ER, Schweingruber FH. 2002. Low-frequency signals in long tree-ring chronologies for reconstructing past temperature variability. *Science* 295: 2250–2253.
- Etzold S, RUEHR N, Zweifel R, Dobbertin M, Zingg A, Pluess P, Häsler R, Eugster W, Buchmann N. 2011. The carbon balance of two contrasting mountain forest ecosystems in Switzerland: similar annual trends, but seasonal differences. *Ecosystems* 14: 1289–1309.
- Fahey T, Woodbury P, Battles J, Goodale C, Hamburg S, Ollinger S, Woodall C. 2009. Forest carbon storage: ecology, management, and policy. *Frontiers in Ecology and the Environment* 8: 245–252.
- Fiedler F. 1986. Die Dendromasse eines hiebsreifen Fichtenbestandes. *Beiträge für die Forstwirtschaft* 20: 171–180.
- Frank D, Esper J. 2005. Characterization and climate response patterns of a high-elevation, multi-species tree-ring network in the European Alps. *Dendrochronologia* 22: 103–122.
- Fritts HC. 1976. *Tree rings and climate*. Caldwell, NJ, USA: The Blackburn Press.
- Gedalof I, Berg A. 2010. Tree ring evidence for limited direct CO₂ fertilization of forests over the 20th century. *Global Biogeochemical Cycles* 24: GB3027.
- Genet H, Breda N, Dufrene E. 2010. Age-related variation in carbon allocation at tree and stand scales in beech (*Fagus sylvatica* L.) and sessile oak (*Quercus petraea* (Matt.) Liebl.) using a chronosequence approach. *Tree Physiology* 30: 177–192.
- Gielen B, De Vos B, Campioli M, Neiryck J, Papale D, Verstraeten A, Ceulemans R, Janssens IA. 2013. Biometric and eddy covariance-based assessment of decadal carbon sequestration of a temperate Scots pine forest. *Agricultural and Forest Meteorology* 174: 135–143.
- Gielen B, Neiryck J, Luysaert S, Janssens I. 2011. The importance of dissolved organic carbon fluxes for the carbon balance of a temperate Scots pine forest. *Agricultural and Forest Meteorology* 151: 270–278.
- Gough C, Vogel C, Schmid H, Curtis P. 2008. Controls on annual forest carbon storage: lessons from the past and predictions for the future. *BioScience* 58: 609–622.
- Granier A, Breda N, Longdoz B, Gross P, Ngao J. 2008. Ten years of fluxes and stand growth in a young beech forest at Hesse, north-eastern France. *Annals of Forest Science* 64: 704.
- Grünwald T, Bernhofer C. 2007. A decade of carbon, water and energy flux measurements of an old spruce forest at the Anchor Station Tharandt. *Tellus* 59: 387–396.
- Hochberg Y. 1988. A sharper Bonferroni procedure for multiple tests of significance. *Biometrika* 75: 800–802.
- Ivesniemi H, Levula J, Ojansuu R, Kolari P, Kulmala L, Pumpanen J, Launiainen S, Vesala T, Nikinmaa E. 2009. Long-term measurements of the carbon balance of a boreal Scots pine dominated forest ecosystem. *Boreal Environmental Research* 14: 731–753.
- Joosten R, Schumacher J, Wirth C, Schulte A. 2004. Evaluating tree carbon predictions for beech (*Fagus sylvatica* L.) western Germany. *Forest Ecology and Management* 189: 87–96.
- Kalliokoski T, Reza M, Jyske T, Mäkinen H, Nojd P. 2012. Intra-annual tracheid formation of Norway spruce provenances in southern Finland. *Trees – Structure and Function* 26: 543–555.
- Kaplan J, Krumhardt K, Zimmerman N. 2012. The effects of land use and climate change on the carbon cycle of Europe over the past 500 years. *Global Change Biology* 18: 902–914.
- Keenan T, Davidson E, Moffat A, Munger W, Richardson A. 2012. Using model-data fusion to interpret past trends, and quantify uncertainties in future projections, of terrestrial ecosystem carbon cycling. *Global Change Biology* 18: 2555–2569.
- Kowalski AS, Loustau D, Berbigier P, Manca G, Tedeschi V, Borghetti M, Valentini R, Kolari P, Berninger F, Rannik Ü *et al.* 2004. Paired comparisons of carbon exchange between undisturbed and regenerating stands in four managed forests in Europe. *Global Change Biology* 10: 1707–1723.
- Kuptz D, Fleischmann F, Matyssek R, Grams T. 2011. Seasonal patterns of carbon allocation to respiratory pools in 60-yr-old deciduous (*Fagus sylvatica*) and evergreen (*Picea abies*) trees assessed via whole-tree stable carbon isotope labeling. *New Phytologist* 191: 160–172.
- Kurz W, Dymond C, Stinson G, Rampley G, Neilson E, Carroll A, Ebata T, Safranyik L. 2008. Mountain pine beetle and forest carbon feedback to climate change. *Nature* 452: 987–990.
- Lapenis A, Lawrence G, Heim A, Zheng C, Shortle W. 2013. Climate warming shifts carbon allocation from stemwood to roots in calcium-depleted spruce forests. *Global Biogeochemical Cycles* 27: 101–107.
- Lasslop G, Reichstein M, Papale D, Richardson A, Arneth A, Barr A, Stoy P, Wohlfahrt G. 2010. Separation of net ecosystem exchange into assimilation and respiration using a light response curve approach: critical issues and global evaluation. *Global Change Biology* 16: 187–208.
- Lindner M, Maroschek M, Netherer S, Kremer A, Barbati A, Garcia-Gonzalo J, Seidl R, Delzon S, Corona P, Kolström M *et al.* 2010. Climate change impacts, adaptive capacity, and vulnerability of European forest Ecosystems. *Forest Ecology and Management* 259: 698–709.
- Litton C, Raich J, Ryan M. 2007. Carbon allocation in forest ecosystems. *Global Change Biology* 13: 2089–2109.
- Lupi C, Morin H, Deslauriers A, Rossi S. 2012. Xylogenesis in black spruce: does soil temperature matter? *Tree Physiology* 32: 74–82.
- Luysaert S, Inglima I, Jung M, Richardson AD, Reichstein M, Papale D, Piao SL, Schulze ED, Wingate L, Matteucci G *et al.* 2007. CO₂ balance of boreal, temperate, and tropical forests derived from a global database. *Global Change Biology* 13: 2509–2537.
- Mäkelä A, Vanninen P. 1998. Impacts of size and competition on tree form and distribution of above-ground biomass in Scots pine. *Canadian Journal of Forest Research* 28: 216–227.

- Mäkinen H. 1999. Effect of stand density on radial growth of branches of Scots pine in southern and central Finland. *Canadian Journal of Forest Research* 29: 1216–1224.
- Melvin T. 2004. *Historical growth rates and changing climatic sensitivity of boreal conifers*. Norwich, UK: PhD thesis, University of East Anglia.
- Moser L, Fonti P, Büntgen U, Esper J, Luterbacher J, Franzen J, Frank D. 2010. Timing and duration of European larch growing season along altitudinal gradients in the Swiss Alps. *Tree Physiology* 30: 225–233.
- Mund M, Kutsch W, Wirth C, Kahl T, Knohl A, Skomarkova M, Schulze ED. 2010. The influence of climate and fructification on the inter-annual variability of stem growth and net primary productivity in an old-growth, mixed beech forest. *Tree Physiology* 30: 689–704.
- Nepal P, Ince P, Skog K, Chang S. 2012. Projection of US forest sector carbon sequestration under US and global timber market and wood energy consumption scenarios, 2010–2060. *Biomass and Bioenergy* 45: 251–264.
- Nickless A, Scholes RJ, Archibald S. 2011. A method for calculating the variance and confidence intervals for tree biomass estimates obtained from allometric equations. *South African Journal of Science* 107: 86–95.
- Ohtsuka T, Mo W, Satomura T, Inatomi M, Koizumi H. 2007. Biometric based carbon flux measurements and net ecosystem production (NEP) in a temperate deciduous broad-leaved forest beneath a flux tower. *Ecosystems* 10: 324–334.
- Ohtsuka T, Saigusa N, Koizumi H. 2009. On linking multiyear biometric measurements of tree growth with eddy covariance-based net ecosystem production. *Global Change Biology* 15: 1015–1024.
- Oleksyn J, Reich P, Chalupka W, Tjoelker M. 1999. Differential above- and below-ground biomass accumulation of European *Pinus sylvestris* populations in a 12-year-old provenance experiment. *Scandinavian Journal of Forest Research* 14: 7–17.
- Pan Y, Birdsey R, Fang J, Houghton R, Kauppi PE, Kurz WA, Phillips OL, Shvidenko A, Lewis SL, Canadell JG *et al.* 2011. A large and persistent carbon sink in the world's forests. *Science* 333: 988–993.
- Papale D, Reichstein M, Aubinet M, Canfora E, Bernhofer C, Kutsch W, Longdoz B, Rambal S, Valentini R, Vesala T *et al.* 2006. Towards a standardized processing of Net Ecosystem Exchange measured with eddy covariance technique: algorithms and uncertainty estimation. *Biogeosciences* 3: 571–583.
- Parresol BR. 1999. Assessing tree and stand biomass: a review with examples and critical comparisons. *Forest Science* 45: 573–593.
- Peichl M, Brodeur J, Khomik M, Arain M. 2010. Biometric and eddy-covariance based estimates of carbon fluxes in an age-sequence of temperate pine forests. *Agricultural and Forest Meteorology* 15: 952–965.
- Pilegaard K, Ibrom A, Courtney M, Hummelshøj P, Jensen N. 2011. Increasing net CO₂ uptake by a Danish beech forest during the period from 1996 to 2009. *Agricultural and Forest Meteorology* 151: 934–946.
- Pöppel B. 1989. *Untersuchungen der Dendromasse in mittelalten Fichtenbeständen*. Forsteinrichtung und Forstliche Ertragskunde, TU Dresden, Germany.
- Pretzsch H. 2000. Die Regeln von Reineke, Yoda und das Gesetz der räumlichen Allometrie. *Allgemeine Forst- und Jagd-Zeitung* 171: 205–210.
- Rannik U, Altimir N, Raittila J *et al.* 2002. Fluxes of carbon dioxide and water vapour over Scots pine forest and clearing. *Agricultural and Forest Meteorology* 111: 187–202.
- Reichstein M, Bahn M, Ciais P, Frank D, Mahecha MD, Seneviratne SI, Zscheischler J, Beer C, Buchmann N, Frank DC *et al.* 2013. Climate extremes and the carbon cycle. *Nature* 500: 287–295.
- Reichstein M, Ciais P, Papale D, Valentini R, Running S, Viovy N, Cramer W, Granier A, Ogée J, Allard V *et al.* 2007. Reduction of ecosystem productivity and respiration during the European summer 2003 climate anomaly: a joint flux tower, remote sensing and modeling analysis. *Global Change Biology* 13: 634–651.
- Reichstein M, Falge E, Baldocchi D *et al.* 2005. On the separation of net ecosystem exchange into assimilation and ecosystem respiration: review and improved algorithm. *Global Change Biology* 11: 1–16.
- Repola J. 2009. Biomass equations for Scots pine and Norway spruce in Finland. *Silva Fennica* 43: 625–647.
- Richardson A, Carbone M, Keenan T, Czimczik C, Hollinger D, Murakami P, Schaberg P, Xu X. 2013. Seasonal dynamics and age of stemwood nonstructural carbohydrates in temperate forest trees. *New Phytologist* 197: 850–861.
- Rocha A, Goulden M, Dunn A, Wofsy S. 2006. On linking interannual tree ring variability with observations of whole-forest CO₂ flux. *Global Change Biology* 12: 1378–1389.
- Sardans J, Penuelas J. 2013. Tree growth changes with climate and forest type are associated with relative allocation of nutrients, especially phosphorus, to leaves and wood. *Global Ecology and Biogeography* 22: 494–507.
- Skomarkova M, Vaganov E, Mund M, Knohl A, Linke P, Boerner A, Schulze ED. 2006. Inter-annual and seasonal variability of radial growth, wood density and carbon isotope ratios in tree rings of beech (*Fagus sylvatica*) growing in Germany and Italy. *Trees* 20: 571–586.
- Skovsgaard J, Nord-Larsen T. 2012. Biomass, basic density and biomass expansion factor functions for European beech (*Fagus sylvatica* L.) in Denmark. *European Journal of Forest Research* 131: 1035–1053.
- Tabacchi G, Di Cosmo L, Gasparini P. 2011. Aboveground tree volume and phytomass prediction equations for forest species in Italy. *European Journal of Forest Research* 130: 911–934.
- Vicca S, Luyssaert S, Peñuelas J, Campioli M, Chapin FS, Ciais P, Heinemeyer A, Höglberg P, Kutsch WL, Law BE *et al.* 2012. Fertile forests produce biomass more efficiently. *Ecology Letters* 15: 520–526.
- Wirth C, Schumacher J, Schulze ED. 2004. Generic biomass functions for Norway spruce in Central Europe – a meta-analysis approach toward prediction and uncertainty estimation. *Tree Physiology* 24: 121–139.
- Wolf A, Field C, Berry J. 2011. Allometric growth and allocation in forests: a perspective from FLUXNET. *Ecological Applications* 21: 1546–1556.
- Wu J, Larsen K, van der Linden L, Beier C, Pilegaard K, Ibrom A. 2013. Synthesis on the carbon budget and cycling in a Danish, temperate deciduous forest. *Agricultural and Forest Meteorology* 181: 94–107.
- Wutzler T, Wirth C, Schumacher J. 2008. Generic biomass functions for Common beech (*Fagus sylvatica*) in Central Europe: predictions and components of uncertainty. *Canadian Journal of Forest Research* 38: 1661–1675.
- Yuste J, Konopka B, Janssens I, Coenen K, Xiao C, Ceulemans R. 2005. Contrasting net primary productivity and carbon distribution between neighboring stands of *Quercus robur* and *Pinus sylvestris*. *Tree Physiology* 25: 701–712.
- Zianis D. 2008. Predicting mean aboveground forest biomass and its associated variance. *Forest Ecology and Management* 256: 1400–1407.
- Zianis D, Menuccini M. 2004. On simplifying allometric analyses of forest biomass. *Forest Ecology and Management* 187: 211–332.
- Zianis D, Muukkonen P, Mäkipää R, Menuccini M. 2005. Biomass and stem volume equations for tree species in Europe. *Silva Fennica* 4: 1–213.
- Zweifel R, Eugster W, Etzold S, Dobbertin M, Buchmann N, Häslar R. 2010. Link between continuous stem radius changes and net ecosystem productivity of a subalpine Norway spruce forest in the Swiss Alps. *New Phytologist* 187: 819–830.

Supporting Information

Additional supporting information may be found in the online version of this article.

Fig. S1 Probability density distributions of the mean wood density measured from each tree at the five study sites.

Fig. S2 De-trended tree-ring width chronologies at the five study sites and the 20 closest sites in the European tree-ring network.

Fig. S3 Percentage difference between wood density corrected and uncorrected total above-ground woody biomass estimates.

Fig. S4 Monthly sums of gross primary productivity at the five study sites.

Fig. S5 Magnitude and inter-annual variability of the eddy-covariance parameters.

Fig. S6 Relationships between tree-ring and eddy-covariance measurements during all possible combinations of months over the previous year April–December period.

Table S1 Critical correlations for different significance levels obtained from a Bonferroni correction to the P values

Please note: Wiley Blackwell are not responsible for the content or functionality of any supporting information supplied by the authors. Any queries (other than missing material) should be directed to the *New Phytologist* Central Office.



About *New Phytologist*

- *New Phytologist* is an electronic (online-only) journal owned by the New Phytologist Trust, a **not-for-profit organization** dedicated to the promotion of plant science, facilitating projects from symposia to free access for our Tansley reviews.
- Regular papers, Letters, Research reviews, Rapid reports and both Modelling/Theory and Methods papers are encouraged. We are committed to rapid processing, from online submission through to publication 'as ready' via *Early View* – our average time to decision is <25 days. There are **no page or colour charges** and a PDF version will be provided for each article.
- The journal is available online at Wiley Online Library. Visit **www.newphytologist.com** to search the articles and register for table of contents email alerts.
- If you have any questions, do get in touch with Central Office (np-centraloffice@lancaster.ac.uk) or, if it is more convenient, our USA Office (np-usaoffice@ornl.gov)
- For submission instructions, subscription and all the latest information visit **www.newphytologist.com**